Reprinted from

MATERIALS SCIENCE & ENGINEERING A

Materials Science and Engineering A226–228 (1997) 142–150

Analysis of crystallization kinetics

Kenneth F. Kelton

Department of Physics, Washington University, St. Louis, MO 63130, USA

ELSEVIER

MATERIALS SCIENCE AND ENGINEERING A

The journal provides an international medium for the publication of theoretical and experimental studies and reviews of the properties and behavior of a wide range of materials, related both to their structure and to their engineering application. The varied topics comprising materials science and engineering are viewed as appropriate for publication: these include, but are not limited to, the properties and structure of crystalline and non-crystalline metals and ceramics, polymers and composite materials.

Types of contributions
Original research work not already published; plenary lectures and/or individual papers given at conferences; reviews of specialized topics within the scope of the journal; engineering studies; letters to the editor.

Subscription Information 1997
Volumes 222–238, each volume containing 2 issues, are scheduled for publication. Prices are available from the publishers upon request. Subscriptions are accepted on a prepaid basis only. Issues are sent by SAL (Surface Air Lifted) mail wherever this service is available. Airmail rates are available upon request.

Orders, claims, and product enquiries: please contact the Customer Support Department at the Regional Sales Office nearest you:

New York
Elsevier Science
P.O. Box 945
New York, NY 10159-0945, USA
Tel.: (+1) 212-633-3730
[Toll free number for North American customers: 1-888-4ES-INFO (437-4636)]
Fax: (+1) 212-633-3680
E-mail: usinfo-f@elsevier.com

Amsterdam
Elsevier Science
P.O. Box 211
1000 AE Amsterdam
The Netherlands
Tel.: (+31) 20-4853757
Fax: (+31) 20-4853432
E-mail: nlinfo-f@elsevier.nl

Tokyo
Elsevier Science
9–15 Higashi-Azabu 1-chome
Minato-ku, Tokyo 106
Japan
Tel.: (+81) 3-5561-5033
Fax: (+81) 3-5561-5047
E-mail: kyf04035@niftyserve.or.ij

Singapore
Elsevier Science
No. 1 Temasek Avenue
#17-01 Millenia Tower
Singapore 039192
Tel.: (65) 434-3727
Fax: (+65) 337-2230
E-mail: asiainfo@elsevier.com.sg

Abstracting and/or Indexing Services
American Ceramic Society; Cambridge Scientific Abstracts; Chemical Abstracts; Current Contents; Engineering Index; FIZ Karlsruhe; Fluid Abstracts; Fluidex; Glass Technology Abstracts; Inspec/Physics Abstracts; Metals Abstracts; Pascal (Centre National de la Recherche Scientifique); Physikalische Berichte; Research Alert™; Science Citation Index.

Advertising information: Advertising orders and enquiries may be sent to: **International**: Elsevier Science, Advertising Department, The Boulevard, Langford Lane, Kidlington, Oxford OX5 1GB, UK. Tel.: (+44)(0)1865 843565. Fax: (+44)(0)1865 843976. **USA and Canada**: Weston Media Associates, Daniel Lipner, P.O. Box 1110, Greens Farms, CT 06436-1110, USA. Tel.: (+1)(203)261-2500. Fax: (+1)(203)261-0101. **Japan**: Elsevier Science Japan, Marketing Services, 1-9-15 Higashi-Azabu Minato-ku, Tokyo 106, Tel: (+81)3-5561-5033; Fax: (+81)3-5561-5047.

ELSEVIER

Materials Science and Engineering A226–228 (1997) 142–150

MATERIALS SCIENCE & ENGINEERING A

Analysis of crystallization kinetics

Kenneth F. Kelton

Department of Physics, Washington University, St. Louis, MO 63130, USA

Abstract

A realistic computer model for polymorphic crystallization (i.e., initial and final phases with identical compositions), which includes time-dependent nucleation and cluster-size-dependent growth rates, is developed and tested by fits to experimental data. Model calculations are used to assess the validity of two of the more common approaches for the analysis of crystallization data. The effects of particle size on transformation kinetics, important for the crystallization of many systems of limited dimension including thin films, fine powders, and nanoparticles, are examined. © 1997 Elsevier Science S.A.

Keywords: Computer modeling; Crystallization kinetics; Microstructure

1. Introduction

An ability to predict and to control the crystallization of metallic and silicate glasses is often critical for the preparation and maintenance of desirable microstructures. Further, the quantitative analysis of kinetic crystallization data can provide information about the magnitude and temperature dependence of nucleation and growth rates, essential parameters for materials design. Kinetic data are generally obtained by monitoring some physical parameter that changes during crystallization, such as the electrical conductivity. The interpretation of such data, however, is often unclear; the electrical resistivity, for example, can be extremely sensitive to the transformation microstructure [1]. The latent heat evolved during crystallization scales linearly with the rate of transformation, making calorimetric measurements such as differential scanning calorimetry (DSC) and differential thermal analysis (DTA) attractive. These techniques are sensitive, relatively easy to make and require small sample quantities. In many cases, however, experimental studies of crystallization suffer from a lack of methods for quantitative analysis. This is particularly true for nonisothermal data, where most methods are based on erroneous assumptions. Even for isothermal studies, however, proper account is frequently not taken of the transformation microstructure, making many conclusions suspect.

Analytical methods for the analysis of isothermal and nonisothermal studies of glass crystallization have been criticized on theoretical and experimental grounds [2–4]. Experimental [5,6] and theoretical [7] studies of the Kissinger method [8], the most commonly used technique for the analysis of nonisothermal data, have demonstrated that it can be used with some confidence for transformations involving growth only. Within this short space it is not possible to review and critique the many analysis schemes that exist; a partial review of these can be found in [2]. Here, a brief review is provided of our studies of polymorphic crystallization of silicate glasses, where the initial and final phases have the same composition. The most common analytical methods of analysis, the Kissinger and Ozawa [9] methods, are examined using this model. It should be emphasized that a silicate glass is chosen only because nucleation and growth rates and required thermodynamic parameters are known; the conclusions drawn also apply to crystallization of metallic glasses.

Accurate data for the time-dependent volume fraction crystallinity are assumed. Experimental details such as proper baseline corrections for calorimetric data are not discussed. Since time-dependent nucleation behavior is central to the model development, this is first reviewed briefly in Section 2.

2. Non-steady-state nucleation rates

Generally, the nucleation rate of crystals in a glass is taken to be constant at the steady-state value, I^s. If true, the number of nuclei produced in a unit volume,

PII S0921-5093(96)10607-9

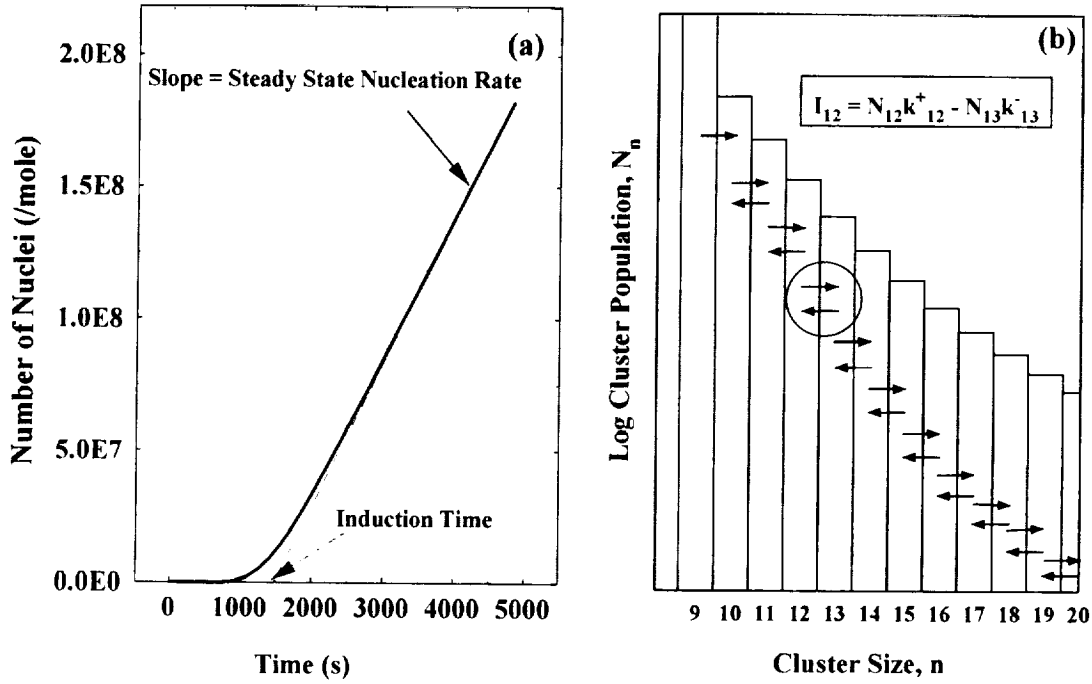

Fig. 1. (a) Number of nuclei as a function of time, illustrating non-steady-state nucleation rates and showing the definition of the induction time; (b) schematic illustration of cluster evolution in the kinetic model for nucleation.

N_v, should then scale linearly with time. In many silicate and some metallic glasses, however, a nonlinear behavior is often found (Fig. 1(a)), which indicates an initially slow nucleation rate that approaches I^s after long annealing times. Such time-dependent, or transient, homogeneous nucleation has been observed in a wide variety of condensed phases [10]; examples of heterogeneous transient nucleation have also been reported in the crystallization of silicate [11] and metallic [12] glasses. Studies of transient nucleation can provide insight into the dynamics of cluster evolution underlying nucleation phenomenon. Further, transient nucleation can determine phase formation and stability [7,13] and often influences the final microstructure.

Time-dependent nucleation can be understood within the classical theory of nucleation [14] where clusters of the new phase grow or shrink by the addition or loss of a single entity (monomer) at a time (Fig. 1(b)), following a series of bimolecular rate reactions. This cluster evolution is described by a system of coupled differential equations of the form:

$$\frac{dN_{n,t}}{dt} = N_{n-1}k^+_{n-1} - (N_{n,t}k^-_n + N_{n,t}k^+_n) + N_{n+1}k^-_{n+1} \quad (1)$$

where k^+_n and k^-_n are the forward and backward rate constants, respectively, which are proportional to the diffusion coefficient in the initial phase, and $N_{n,t}$ is the number of clusters at time t containing n monomers.

The rates and cluster densities are governed by the work of cluster formation, W_n, which for spherical clusters containing n monomers and having a sharp interface with the initial phase can be written approximately as

$$W_n = n\delta\mu + (36\pi)^{1/3}\bar{v}^{2/3}n^{2/3}\sigma \quad (2)$$

where $\delta\mu$ is the Gibbs free energy per monomer of the new phase less that of the initial phase, $\bar{v}$ is the molecular volume and σ is the interfacial energy per unit area. The nucleation rate, $I_{n,t}$, is defined as the flux in cluster-size space; in the most general case, it is a function of both time and the cluster size at which it is measured,

$$I_{n,t} = N_{n,t}k^+_n - N_{n+1,t}k^-_{n+1} \quad (3)$$

Given sufficient time, the cluster density evolves by the mechanism described in Eq. (1) and approaches a constant value, the steady-state distribution, $N^s_{n,t}$, producing a constant, steady-state rate. Since many metallic and silicate glasses are formed by rapid quenching from the melt, there is often insufficient time to maintain this steady-state distribution of clusters, however, resulting in a final cluster distribution that is more similar to that at a higher temperature, having a lower cluster density at the critical size and therefore a depressed nucleation rate. With time, the distribution evolves to the steady-state one, giving rise to the characteristic time-dependent nucleation rate.

3. Johnson–Mehl–Avrami–Kolmogorov (JMAK) analysis

In the very early stages of polymorphic crystallization (i.e., no compositional change) of glasses, overlap between the different transformed regions can be ignored and the volume fraction crystallized can be written as

$$x_e = \frac{4\pi}{3V_0}\int_0^t I(\tau)\left[\int_\tau^t g(t')\,dt'\right]^3 d\tau \quad (4)$$

Here, V_0 is the sample volume, $I(\tau)$ is the time-dependent nucleation rate and $g(t')$ is the time-dependent growth rate. As the crystallized regions become larger, they eventually impinge and alter the transformation kinetics. If the sample size is much greater than any individual transformed region and if growth proceeds homogeneously throughout the sample, with spatially random nucleation, then the effect of impingement on the kinetics can be computed statistically to yield the familiar JMAK expression [15,16], i.e., $x(t) = 1 - \exp(-x_e(t))$. For interface-limited growth and a constant nucleation rate:

$$x(t) = 1 - \exp(-4\pi I g^3 t^4/3V_0) \quad (5)$$

Often, a general form of this type is assumed to describe isothermal phase transformations in other cases:

$$x(t) = 1 - \exp(-(kt)^n) \quad (6)$$

The parameters describing the reaction kinetics, such as the nucleation and growth rates, are now contained within an effective kinetic parameter, k, while the exponent, n, called the Avrami exponent, provides some information about the dimensionality of the transformation, i.e., whether it is one-, two- or three-dimensional and whether it is interface-limited or diffusion-limited. A simple manipulation of Eq. (6) shows that for isothermal cases, these values are determined by plotting the measured data, $x(t)$, as

$$\ln\left[\ln\left(\frac{1}{1-x(t)}\right)\right] = n\ln(k) + n\ln(t) \quad (7)$$

A plot of $\ln[\ln(1-x)^{-1}]$ versus $\ln(t)$ should then give a straight line with slope n and intercept $n\ln(k)$.

Continuously curved lines in Avrami plots have led to attached importance for 'local values' of the Avrami exponent [17]. Generally, however, such behavior signals a violation of a fundamental assumption of the JMAK theory. A familiar example in crystals is grain boundary nucleation which violates the assumption of spatially random nucleation [18], for example. Examples of similar violations in glass devitrification include surface crystallization [1] and an inhomogeneous distribution of quenched in nuclei [19]. It is important to note that when applied in situations consistent with the original assumptions, the JMAK analysis is valid.

4. Finite sample size effects

Samples for DSC/DTA studies are often small, in the form of powders, thin films or ribbons. For rapid nucleation in reasonably large samples, possible finite-size effects on the transformation kinetics can be ignored. For low nucleation rates, however, or extremely small sample sizes, as for non-consolidated nanoparticles, the size of an individual transforming region is of order the size of the sample, thus violating a fundamental assumption of the JMAK analysis. Possible effects on the crystallization kinetics have been considered only recently [20–22].

The probability for nucleation in small samples is readily obtained using Poisson statistics; growth presents a more difficult problem. Given a small ensemble of crystallizing regions and assuming isotropic growth, some crystallites will intersect the sample surface prior to complete transformation and growth will cease, thus violating the assumption of unimpeded growth that led to the JMAK equation. A recent study [21] shows that if the regions of significant nucleation and growth do not overlap (valid for many silicate glasses) the finite-size-corrected volume fraction transformed from N nuclei can be written approximately in terms of a scaled time, κ,

$$x(t) = 1 - \exp\left[-N\left(\kappa(t)^3 - \frac{9}{16}\kappa(t)^4 + \frac{m(N)}{32}\kappa(t)^6\right)\right] \quad (8)$$

where $\kappa = gt/R$, g being the growth velocity of the crystal region, R the sample particle radius, and t the time; $m(N)$ is equal to the larger of the two quantities (5.26–0.26 N) or 1. Particle shape effects are easily included, using an effective value for $\kappa^e = (V_e/V_0)^{1/3}$, where V_e is the extended volume of a growing crystallite and V_0 is the volume of the sample. Predictions from Eq. (8) agree with computer simulations of the transformation of a finite ensemble of noninteracting spins on a lattice (Fig. 2(a)–(c)), while those from the JMAK expression compare poorly. The Avrami exponent obtained by a fit of the JMAK equation to the finite-size-corrected data (Fig. 2(d)) is initially low, due to the inapplicability of the JMAK analysis, and approaches the expected value of $n = 3$ as the number of clusters becomes large.

5. Realistic computer model for isothermal and nonisothermal crystallization

A computer model of polymorphic crystallization that includes time-dependent nucleation, cluster-size-dependent growth rates and finite-size effects is developed and applied to the crystallization of lithium disilicate glass.

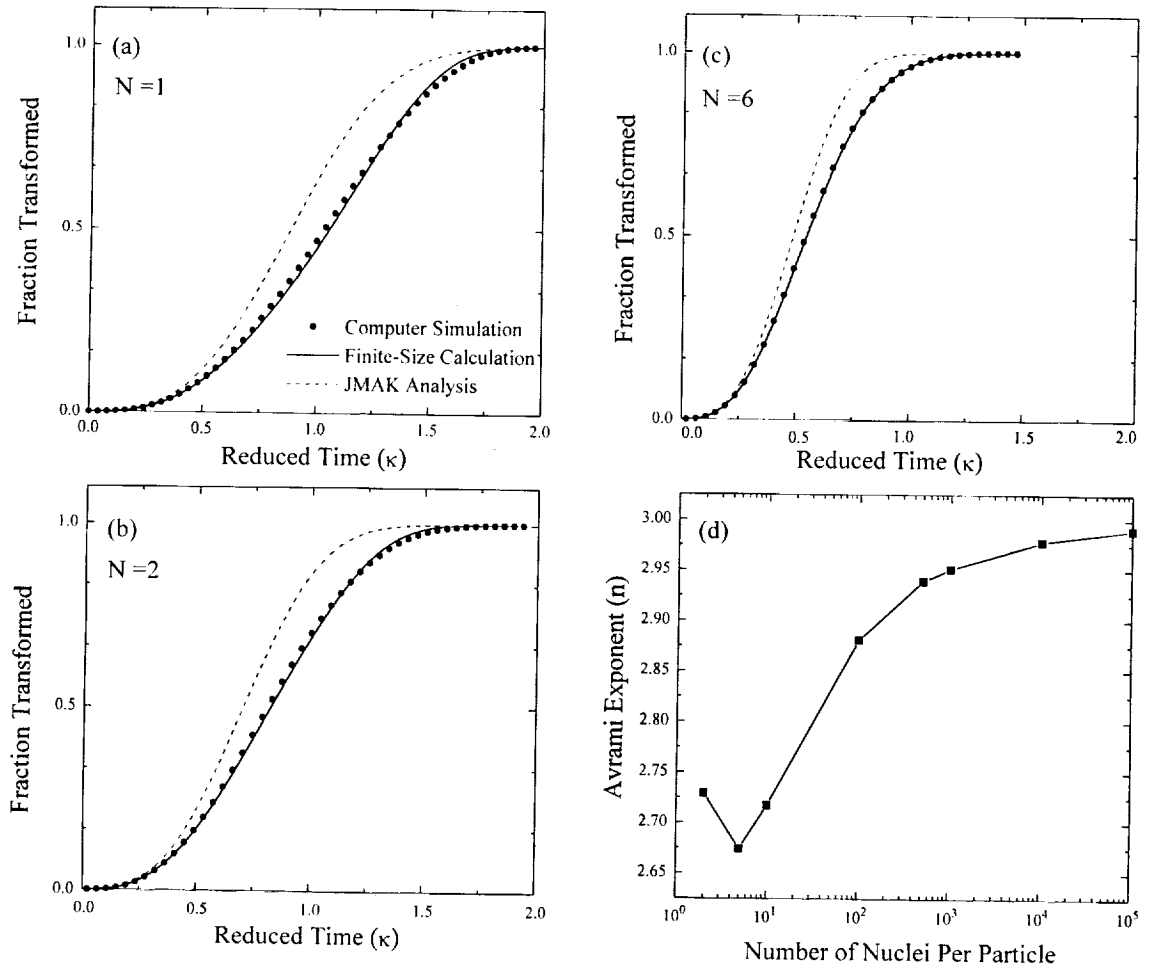

Fig. 2. The fraction transformed as a function of reduced time, κ, for (a) one, (b) two and (c) six crystallites in a particle ((a) (c) taken from [21]). The simulation results were obtained on a spherical lattice of radius 50 units. Eq. (8) is used for the finite-size calculation, which provides the best fit to the lattice simulation. (d) The Avrami exponent computed from a JMAK analysis of the finite-size-corrected data.

5.1. Development of computer model

The transformation time is divided into a series of short isothermal intervals of duration Δt, over which new nuclei appear and previously generated ones grow. The coupled differential equations (i.e., Eq. (1)) are solved using a finite difference method [23], in which each isothermal interval is divided into a large number of smaller intervals, δt, and the number of clusters of size n at the end of each interval is computed by

$$N_{n,t+\delta t} = N_{n,t} + \delta t \frac{\mathrm{d}N_{n,t}}{\mathrm{d}t} \tag{9}$$

where $\mathrm{d}N_{n,t}/\mathrm{d}t$ is given by Eq. (1). Given $N_{n,t}$, the time-dependent nucleation rate is computed directly using Eq. (3). By this method, no assumptions of thermal history are made. At the end of each Δt interval, nuclei generated in previous intervals are grown assuming a size-dependent growth rate [13]:

$$g(R) = C\frac{16D}{\lambda^2}\left(\frac{3\bar{v}}{4\pi}\right)^{1/3}\sinh\left[\frac{\bar{v}}{2kT}\left(\Delta G_v - \frac{2\sigma}{r}\right)\right] \tag{10}$$

Here, k is Boltzmann's constant, λ is the jump distance, and ΔG_v is the change in Gibbs free energy per volume of the new phase less that of the initial phase. For nonisothermal transformations, the duration of the isothermal interval, Δt, is inversely related to the scan rate, S. The extended volume fraction transformed, x_e, is calculated at the end of each interval by summing over all previous m intervals:

$$x_e(t,T) = \frac{1}{V_0}\sum_{i=1}^{m}\left(\frac{4\pi}{3}\right)N_i r_{i,t}^3 \tag{11}$$

Finite-size effects are included as discussed in Section 4. Since for many silicate glasses, the nucleation and growth are well separated, all crystallites are approximately the same size, allowing the scaled time, κ^e, to be obtained directly from the extended volume fraction for an infinite system, $x_\infty^e(t)$, i.e., $\kappa^e = (x_\infty^e(t)/N)^{1/3}$. Surface crystallization is frequently important for silicate and

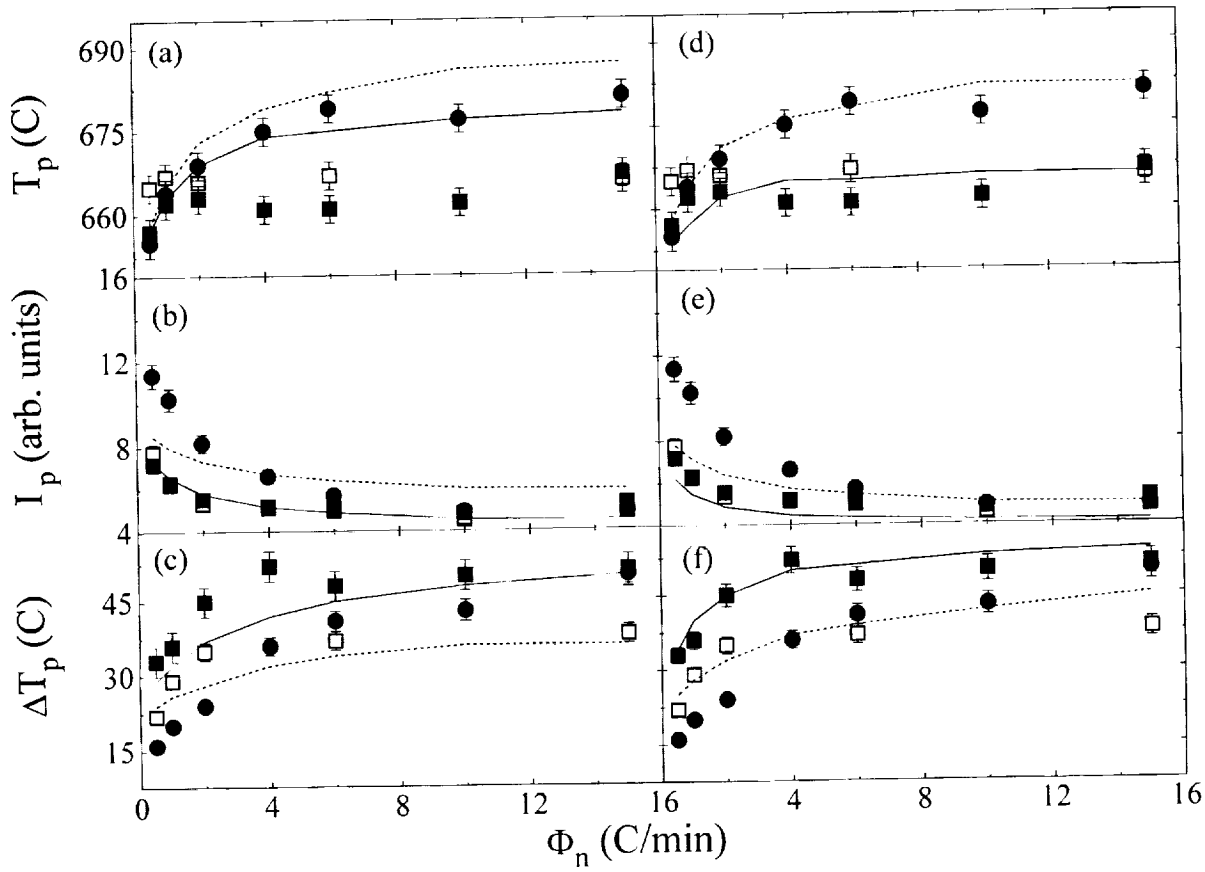

Fig. 3. The effect of scanning through the nucleation zone at different rates on the DSC/DTA peak parameters. For 425–450 particles: data (■) and (□); calculation (——). For 850–1170 particles: data (●); calculation (– – –). Calculations in (a) and (c) are for spherical particles; (d) (e) assume ellipsoidal particles with eccentricity (1, $\frac{1}{2}$, $\frac{1}{2}$) (from [25]).

metallic glasses. For the glass studied here, surface nucleation is sufficiently rapid that the nucleation step can be ignored [24]; the rate of transformation due to a spherical growth front originating on the surface can then be assumed. Taking the growth velocity for the shell as constant and equal to that predicted from Eq. (10) as $r \to \infty$, $g(\infty)$, the volume fraction transformed by surface growth alone is

$$x_s = \left[1 - \left(\frac{R - g(\infty)t}{R}\right)^3\right] \tag{12}$$

Calculating the volume transformed by surface growth, and taking account of the overlap between surface, x_s, and volume, x_v, crystallization, the time-dependent volume transformed is given by

$$x(t) = x_s + x_v(1 - x_s) \tag{13}$$

Assuming that the rate of change of the enthalpy, dH/dt scales linearly with the rate of volume transformed, the DSC/DTA signal can then be computed as a function of time and/or temperature as

$$\text{DSC Signal:} \quad \propto \frac{x(T_i + \delta T) - x(T_i)}{\delta t} \tag{14}$$

5.2. Application to crystallization of lithium disilicate glass

Measured parameters were assumed to model the crystallization of lithium disilicate glass. The fitting parameters were held constant at the values determined from direct nucleation and growth data; they were not optimized to produce better agreement with the experimental data for crystallization. DSC/DTA peak parameters, such as peak temperature, T_p, and peak height, I_p, are strong functions of particle size [24] and sample history; the computer model presented here is capable of taking both effects into account. As an example, Fig. 3 compares the model predictions with experimental data for peak parameters for two sizes of spherical glass particles that were first scanned through the region in which the nucleation rate is significant (400–500°C) at rates, Φ_n, between 2 and 15°C min^{-1}, and were subsequently scanned through the crystallization peak at a rate, Φ_c, of 15°C min^{-1}. Symbols are used for the data; the lines are the calculations. Results from two independent DSC/DTA measurements of these glasses are presented, providing a measure of the

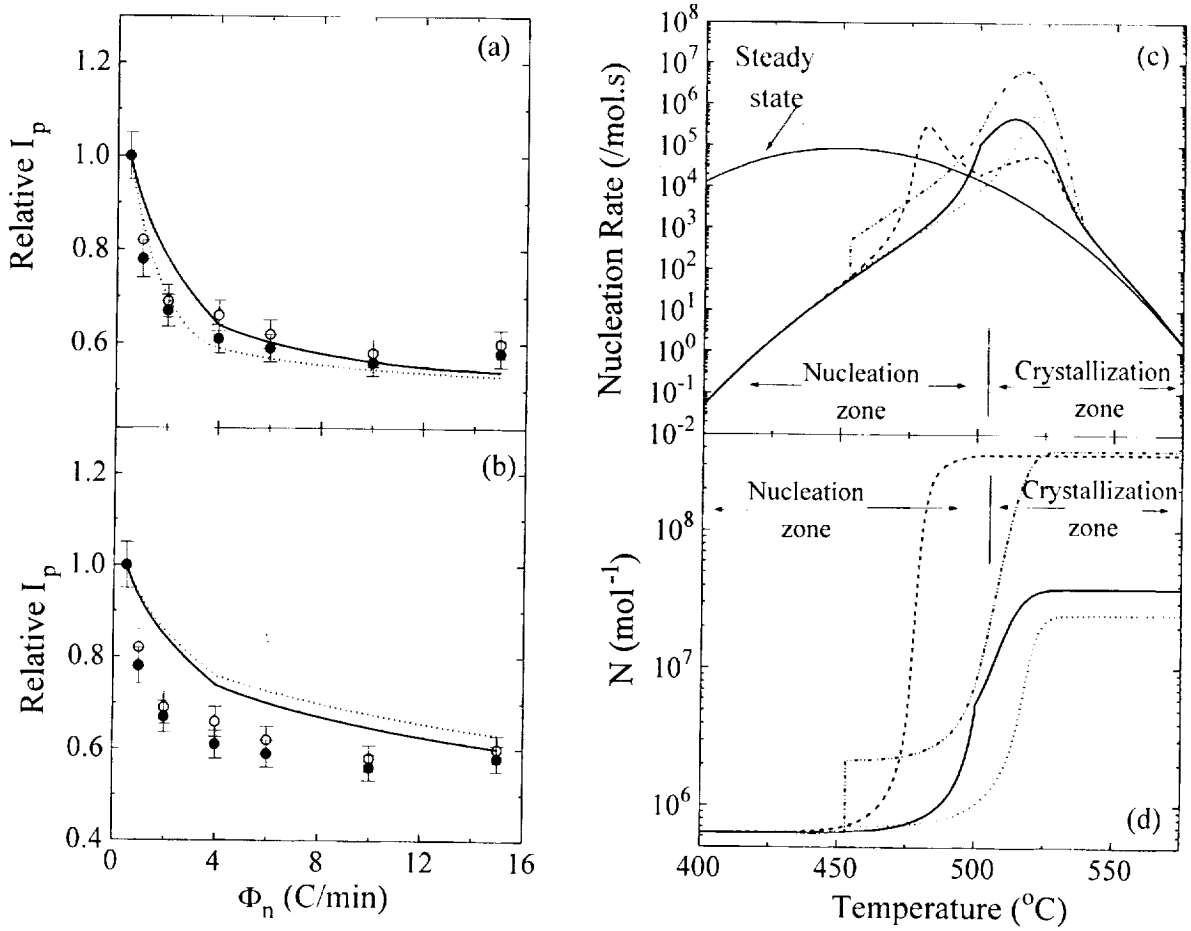

Fig. 4. (a) and (b): Calculated relative peak heights, I_p, for glasses that had been scanned through the nucleation zone (——) or held isothermally for a corresponding amount of time at the peak temperature of the steady-state rate (- - -) compared with experimental data ((●) scanned glasses; (○) isothermally treated glasses). Calculations in (a) were made assuming transient nucleation; steady-state rates were assumed for (b). Corresponding calculated time-dependent nucleation rates are shown in (c) and total number of nuclei in (d). The solid and dashed lines are for samples scanned through the nucleation zone at $\Phi_n = 4$ and 0.5°C min^{-1}, respectively; the dotted and dot-dot-dash lines are for samples annealed at the peak nucleation temperature for 18.75 and 150 min, respectively. The steady-state nucleation rate is also shown and the nucleation and crystallization zones are indicated.

experimental error. Though the predicted trends for spherical particles (Fig. 3(a)–(c)) follow the data, slightly improved agreement is obtained if ellipsoidal particles are assumed (Fig. 3(d)–(f)). Optical microscopy studies of the particles show that this assumption is reasonable.

Time-dependent nucleation can significantly enhance glass formation [13] and glass stability [7], due to the smaller number of quenched-in nuclei. As is illustrated in Fig. 4, however, the inherited non-steady-state cluster distribution can also result in unexpected transformation behavior. Here the computed and experimentally measured DSC/DTA peak heights are compared for glasses that were either first scanned through the nucleation zone (400–500°C), or annealed isothermally at the peak temperature for an amount of time equal to that required to scan over the range of significant nucleation (425–500°C). Both sets of glasses were subsequently scanned through the DSC/DTA peak at 15°C min^{-1}. The measured peak heights are approximately equal, but fall faster than predicted from steady-state calculations (Fig. 4(b)), indicating a stronger dependence on the number of nuclei produced than expected from the temperature dependence of the steady-state rate alone. The experimental and calculated results are almost indistinguishable from the time-dependent nucleation calculation (Fig. 4(a)).

Earlier calculations by us predicted that if transient nucleation effects were important, the nucleation rate could rise above the steady-state nucleation rate during nonisothermal devitrification, peaking at a temperature higher than the peak of the steady-state rate [7]. A similar behavior is expected here following both isothermal and nonisothermal anneals (Fig. 4(c)); two peaks are even predicted when $\Phi_n = 0.5$°C min^{-1}. Fig. 4(d) shows the number of nuclei produced as a function of temperature for different annealing treatments; this complex behavior is a result of the relaxation of the

cluster distribution inherited from the quench. From steady-state arguments, the number of nuclei should scale linearly with the annealing time in the nucleation zone; the predicted time-dependent behavior is more complicated. For example, for $\Phi_n = 0.5°C\ min^{-1}$, most of the nucleation occurs in the nucleation zone. Though approximately the same number of nuclei are produced for the corresponding case of a 150 min anneal at the peak temperature of the steady-state rate, these are nucleated at a temperature above the upper limit of the nucleation zone. Anneals within the nucleation zone then directly produce nuclei, but equally important, they result in differing degrees of relaxation of the cluster distribution toward the steady state one. The observed agreement between the isothermal and non-isothermal annealing treatments is therefore only fortuitous. It is, however, a dramatic demonstration of the often subtle effects of time-dependent nucleation on phase formation and stability. This also further demonstrates that simple interpretations of DSC/DTA data, even in apparently simple situations, are often not possible.

5.3. Critique of Kissinger and Ozawa analysis techniques

Having established the validity of the model, it can be used to make meaningful evaluations of commonly used methods of analysis for DSC/DTA data. Peak profiles for DSC/DTA data were first computed using known kinetic and thermodynamic parameters for lithium disilicate glass. These data were then analyzed in the usual way and the derived parameters were compared with those used for the calculations. Two method of analysis for DSC/DTA data are most common. The Kissinger method [8],

$$\frac{d\ln\left(\frac{Q}{T_p^2}\right)}{d\left(\frac{1}{T_p}\right)} = -\frac{E}{R} \tag{15}$$

where Q is the DSC scan rate and T_p is the peak temperature (K), is often used to estimate the effective activation energy of the transformation, E. The Ozawa method [9]

$$\left.\frac{d(\log[\ln(1-x)])}{d\log Q}\right|_T = -n \tag{16}$$

is used to estimate the Avrami coefficient, n, which can provide information about the transformation mechanism. The validity of these expressions was checked by application to numerically generated DSC/DTA transformation peaks for computed, quenched, glasses using known thermodynamic and kinetic parameters. DSC/DTA data were generated for infinite samples and for cases where surface and finite-size effects were included. In all cases, straight lines were obtained for the Kissinger and Ozawa plots. As illustrated in Fig. 5(a), the activation energies obtained from Kissinger plots of the computed DSC/DTA data (given by the slopes of the lines) were a strong function of the sample thermal history and whether surface and sample size effects were included. Large values of n were obtained from an Ozawa analysis of the more rapidly quenched glasses, indicating that time-dependent nucleation is dominant during the transformation. A value of n near 3 for the glasses quenched at $0.01°C\ s^{-1}$ suggests that the transformation proceeds primarily by growth on quenched-in nuclei. This was verified by noting that the activation energies computed from a Kissinger analysis become more similar (Fig. 5(a)), and the Avrami coefficients approach 3 for all glasses that were first saturated with nuclei by annealing in the nucleation zone (400–500°C).

Since nucleation and growth are widely separated in temperature for lithium disilicate glass, the activation energies obtained from a Kissinger analysis should be related to those of the growth rate, particularly if it is described by an Arrhenius temperature dependence. For the more realistic non-Arrhenius growth rates in this glass, however, the situation is more complicated. As illustrated in Fig. 5(b), showing the local activation energy for growth as a function of temperature, activation energies obtained by a Kissinger analysis correspond roughly to the average value of the activation energy over the range of transformation temperatures for the different scan rates, though the value is not located precisely at the midpoint of the range. As illustrated, changes in the activation energy resulting from the introduction of finite-size effects or from thermal annealing are due to a change in the temperature range of transformation. Samples of finite-size are transformed at lower temperatures due to a more rapid transformation of the finite volume while low temperature annealing simply results in more nuclei that collectively transform the sample earlier. Even for this relatively simple case of polymorphic crystallization with separation between nucleation and growth, a proper interpretation of activation energies derived from a Kissinger analysis is difficult to make, particularly when information is desired about the influence of nucleation from anneals below the DSC/DTA transformation temperature. For cases where the nucleation and growth regions overlap considerably, a Kissinger analysis gives meaningless results. Since the nucleation rate has a strongly non-Arrhenius temperature dependence, a primary assumption of the derivation is violated. Because the Ozawa method avoids this assumption, the estimated Avrami coefficient more accurately reflects the importance of nucleation at temperatures below the transition temperature in the most rapidly quenched glasses.

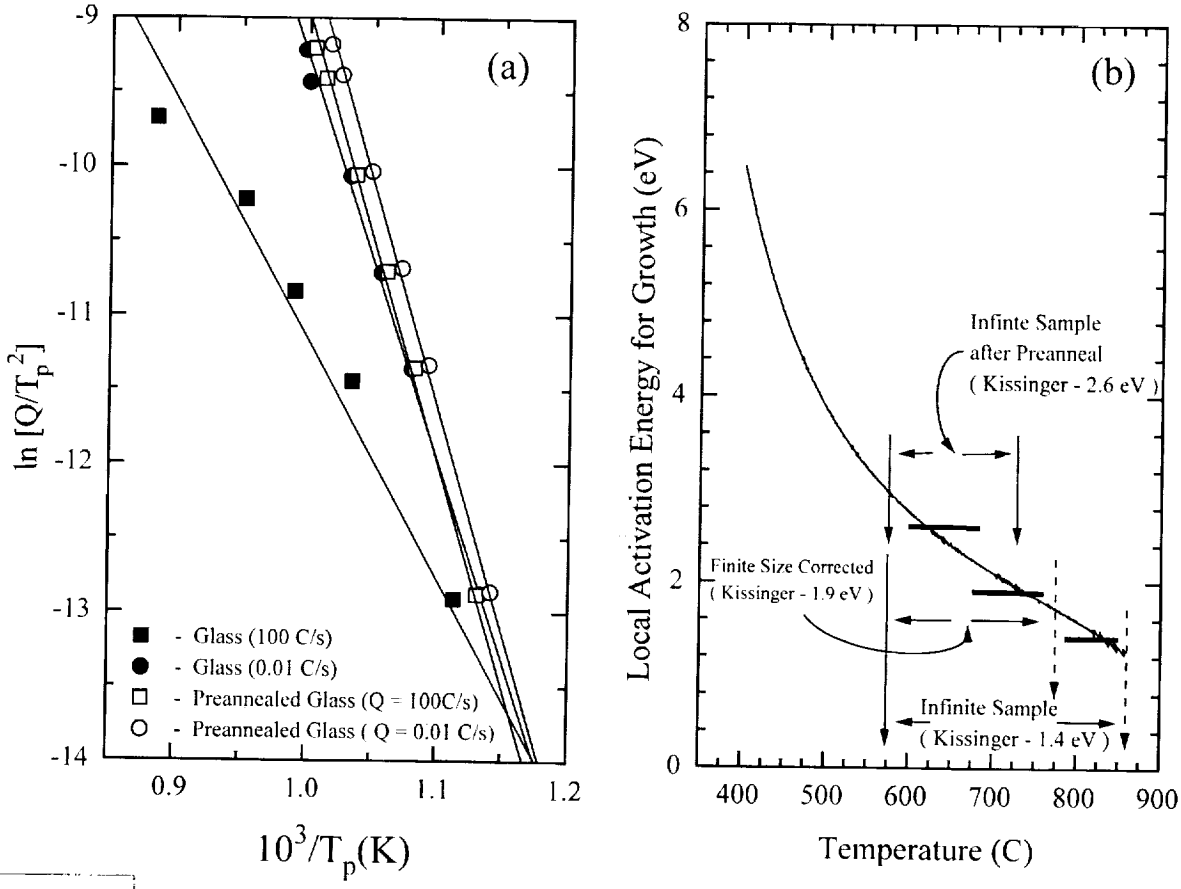

Fig. 5. (a) Kissinger analysis for as-quenched glasses and glasses that had been annealed in the nucleation zone (400–500°C); (b) local activation energy for growth velocity.

Most techniques for the analysis of nonisothermal crystallization data rely on similar assumptions to those made for the Kissinger analysis and therefore have the same level of validity. How then can this data be better analyzed? As discussed in Section 5.2, it should be possible to distinguish between crystallization mechanisms based on a qualitative analysis of the peak shapes. An iterative computer fit to the peak parameters, using supplemental information of the transforming microstructure, can therefore yield quantitative kinetic information. Computer modeling can also be used to devise and establish levels of confidence for methods that allow quick estimates to be made of important parameters for processing, such as the extent of the nucleation zone [26,27].

6. Conclusions and future directions

A brief discussion of the polymorphic crystallization of glasses was presented. A new approximate expression for finite-sample size effects on the transformation kinetics was discussed and was incorporated into a computer-based model for isothermal and nonisothermal crystallization data. Good agreement between model predictions and experimental data the crystallization of lithium disilicate glass was demonstrated. Though a silicate glass was used for discussion, the general conclusions follow for all cases of polymorphic devitrification. Primary conclusions include the following:

- the JMAK analysis is correct when applied within its range of validity;
- for widely separated nucleation and growth regimes, common for silicate glasses, the Kissinger analysis of polymorphic crystallization data can provide an estimate of the activation energy for growth, but is invalid otherwise;
- the Ozawa analysis gives reasonable estimates of the Avrami exponent for polymorphic transformations;
- time-dependent nucleation can result in complicated devitrification behavior that cannot be understood with any simple method of analysis—realistic computer modeling is required;
- a detailed study of the peak shape in DSC/DTA data can give more quantitative information than can be obtained from Kissinger-type methods;

- supplementary information of the transformation microstructure must be incorporated into any analysis of calorimetric data.

The results presented here were for polymorphic devitrification by homogeneous nucleation. Clearly, they should be extended to the more common case of primary crystallization. Though diffusion-limited growth has been well studied and can be incorporated into the computer model in a rather straightforward manner, the correct treatment for the time-dependent nucleation of a cluster with a composition different from that of the parent phase is unclear. Here the embryo composition can change with cluster size and the chemical make-up of the regions surrounding the embryos will likely vary in a complicated manner, given the stochastic nature of cluster evolution. Often the classical theory can still be applied, changing only the Gibbs free energy [28,29] or the interfacial energy [30] with composition. When competition between diffusion in the parent phase and interfacial attachment arises, however, the classical theory is inadequate because the diffusive fluxes in the parent phase are coupled into the stochastic fluxes from the parent phase to clusters of the new phase. We have recently extended our model of time-dependent nucleation to treat this latter case. Interestingly, the scaling of the nucleation rate and the transient time with the mobility as obtained from the classical theory changes. A more complex dependence on thermal history is therefore predicted, likely making the use of simple analytical expressions, such as the Kissinger analysis, even more invalid.

Crystallization studies are rich, particularly when coupled with multi-step annealing treatments. More realistic models, such as the computer model described here, however, are required for the proper analysis of these data. The ready availability of the necessary computer processing power now makes this feasible.

Acknowledgements

This work was partially supported by NASA under contracts NAG 8-898 and NCC-849.

References

[1] K.F. Kelton and F. Spaepen, *Acta Metall.*, *3* (1985) 455.
[2] H. Yinnon and D.R. Uhlmann, *J. Non-Cryst. Solids*, *54* (1983) 253.
[3] L. Granasy and T. Kemeny, *Thermochimica Acta*, *42* (1980) 289; T. Kemeny and L. Granasy, *J. Non-Cryst. Solids*, *68* (1984) 193.
[4] M.C. Weinberg, *J. Non-Cryst. Solids*, *82* (1987) 779.
[5] C.S. Ray and D.E. Day, *J. Am. Ceram. Soc.*, *73* (1990) 430.
[6] X.J. Xu, C.S. Ray and D.E. Day, *J. Am. Ceram. Soc.*, *74* (1991) 909.
[7] K.F. Kelton, *J. Non-Cryst. Solids*, *163* (1993) 283.
[8] H.E. Kissinger, *Anal. Chem.*, *29* (1957) 1702; D.W. Henderson, *J. Non-Cryst. Solids*, *30* (1979) 301.
[9] T. Ozawa, *Polymer*, *12* (1971) 150.
[10] K.F. Kelton, *Mater. Sci. Eng.*, *B32* (1995) 145.
[11] K. Lakshmi Narayan, K.F. Kelton and C.S. Ray, *J. Non-Cryst. Solids*, *195* (1996) 148.
[12] U. Koster and M. Blank-Bewersdorff, *MRS Symp. Proc.*, *57* (1987) 115.
[13] K.F. Kelton and A.L. Greer, *J. Non-Cryst. Solids*, *180* (1986) 17.
[14] K.F. Kelton, in *Solid State Physics*, Academic Press, New York, 1991, pp. 75–177.
[15] A.N. Kolmogorov, *Isz. Akad. Nauk SSR, Ser. Fiz.*, *3* (1937) 355.
[16] W.A. Johnson and R. Mehl, *Trans. AIME*, *135* (1939) 416; M. Avrami, *J. Chem. Phys.*, *7* (1939) 1103.
[17] A. Calka and A.P. Radlinski, *Mater. Sci. Eng.*, *97* (1988) 241.
[18] J.W. Cahn, *Acta Metall.*, *4* (1956) 449.
[19] J.C. Holzer and K.F. Kelton, *Acta Metall.*, *39* (1991) 1833.
[20] M.C. Weinberg, *J. Non-Cryst. Solids*, *142* (1992) 126.
[21] L.E. Levine, K. Lakshmi Narayan and K.F. Kelton, *J. Mater. Res.*, *12* (1997) 124.
[22] J.W. Cahn, in J.S. Im, B. Park, A.L. Greer and G.B. Stephenson (Eds.), *MRS Symp. Proc.*, Vol. 38, 1996, pp. 425–438.
[23] K.F. Kelton, A.L. Greer and C.V. Thompson, *J. Chem. Phys.*, *79* (1983) 6261.
[24] W.S. Huang, C.S. Ray, D.E. Day, K.L. Narayan, T.C. Cull and K.F. Kelton, *J. Non-Cryst. Solids*, *204* (1996) 1.
[25] K.F. Kelton, K.L. Narayan, L.E. Levine, T.C. Cull and C.S. Ray, *J. Non-Cryst. Solids*, *204* (1996) 13.
[26] C.S. Ray and D.E. Day, *J. Am. Ceram. Soc.*, *73* (1990) 439.
[27] K.F. Kelton, *J. Am. Ceram. Soc.*, *75* (1992) 2449.
[28] J.H. Perepezko and J.S. Smith, *J. Non-Cryst. Solids*, *44* (1981) 65.
[29] C.V. Thompson and F. Spaepen, *Acta Metall.*, *31* (1983) 2021.
[30] K.F. Kelton and K. Lakshmi Narayan, *J. Non-Cryst. Solids*, submitted.

Instructions for Authors

SUBMISSION OF PAPERS

Manuscripts for the main part of the journal and for the Letters Section should be submitted as follows:

For authors in Europe

Editor-in-Chief
Professor Herbert Herman
Department of Materials Science and Engineering
State University of New York at Stony Brook
Long Island, NY 11794-2275
USA
Fax: +1 (516) 632 8052

or

Professor Gernot Kostorz
ETH Zurich
Institut für Angewandte Physik
CH-8093 Zurich
Switzerland
Fax: +41 (1633) 1105

For authors in Japan

Professor Masahiro Koiwa
Department of Materials Science and Engineering
Faculty of Engineering
Kyoto University
Yoshida-Honmachi, Sakyo-ku
Kyoto 606-01
Japan
Fax: +81 (75) 751 7844

For authors in North and South America and the rest of the world

Professor Herbert Herman
USA

or

Professor Carl C. Koch
North Carolina State University
Department of Materials Science and Engineering
233 Riddick Building
Yarbrough Drive
Raleigh, NC 27695-7907
USA
Fax: +1 (919) 515 7724

Manuscripts

Three copies should be submitted to the Editor, in double-spaced typing on pages of A4 size and with wide margins (Letters should not exceed 2000 words and a maximum of 5 figures). All tables and illustrations should bear a title or legend.
An *abstract* should accompany reviews, original papers and Letters. It should present (preferably in 100–150 words; 50 words or less for Letters) a brief and factual account of the contents and conclusions of the paper, and an indication of the relevance of new material.
References should be indicated by numerals in square brackets, introduced consecutively and appropriately in the text.

References must be listed on separate sheet(s) at the end of the paper. Every reference appearing in the text should be quoted in the reference list, and *vice versa*. When reference is made to a publication written by more than two authors it is preferable to give only the first author's name in the text followed by "*et al.*" However, in the list of references the names and initials of all authors must be given.
Three sets of figures should be submitted. One set of line drawings should be in a form suitable for reproduction, drawn in Indian ink on drawing or tracing paper (letter height, 3–5 mm). Alternatively, such illustrations may be supplied as high contrast, black-and-white glossy prints. Duplicate original micrographs should be provided wherever possible to facilitate the refereeing process. Magnifications should be indicated by a ruled scale bar on the micrograph. Captions to illustrations should be typed in sequence on a separate page.
All abbreviated terms must be defined when first used (both in the abstract and in the text) and authors must express all quantities in SI units, with other units in parentheses if desired.
Authors in Japan please note that information about how to have the English of your paper checked, corrected and improved (before submission) is available from:
Elsevier Science Japan
Higashi-Azabu 1-chome Building 4F
1-9-15 Higashi-Azabu
Minato-ku
Tokyo 106
Japan
Tel: +81-3-5561-5032; Fax: +81-3-5561-5045.

Further information

All questions arising after the acceptance of manuscripts, especially those relating to proofs, should be directed to:
Elsevier Editorial Services
Mayfield House
256 Banbury Road
Oxford OX2 7DH
UK
Tel. +44(0) 1865 314900; Fax. +44(0) 1865 314990.

Submission of electronic text

The final text may be submitted on a 3.5 in or 5.25 in diskette (in addition to a hard copy with original figures). Double density (DD) or high density (HD) diskettes are acceptable, but must be formatted to their capacity before the files are copied on to them. The main text, list of references, tables and figure legends should be stored in separate text files with clearly identifiable file names. The format of these files depends on the word processor used. WordPerfect 5.1 is the most preferable but for other formats please refer to the Instructions to Authors booklet. It is *essential* that the name and version of the wordprocessing program, type of computer on which the text was prepared, and format of the text files are clearly indicated.
The final manuscript may contain last minute corrections which are not included in the electronic text but such corrections must be clearly marked on the hard copy.